IET Signal Processing

Review Article

IET Journals
The Institution of Engineering and Technology

Survey of CSI fingerprinting-based indoor positioning and mobility tracking systems

ISSN 1751-9675
Received on 22nd January 2020
Revised 29th April 2020
Accepted on 18th May 2020
E-First on 14th July 2020
doi: 10.1049/iet-spr.2020.0028
www.ietdl.org

Josyl Mariela Rocamora[1,2], Ivan Wang-Hei Ho[1] ✉, Wan-Mai Mak[1], Alan Pak-Tao Lau[3]

[1]Department of Electronic and Information Engineering, The Hong Kong Polytechnic University, Kowloon, Hong Kong
[2]Department of Electronics Engineering, University of Santo Tomas, Manila, Philippines
[3]Department of Electrical Engineering, The Hong Kong Polytechnic University, Kowloon, Hong Kong
✉ *E-mail: ivanwh.ho@polyu.edu.hk*

Abstract: Techniques for indoor positioning systems (IPSs) can be categorised as range-based or range-free. Range-based methods rely on geometric mappings to approximate a location given the calculated distances or angles from multiple reference points. In contrast, range-free strategies utilise fingerprinting, wherein an acquired fingerprint data is compared to a pre-collected dataset to identify the best position estimate. Among these, fingerprinting of channel state information (CSI) is preferred over other information such as received signal strength indicator as the former can exploit the effect of multipath propagation and is robust against non-line-of-sight channels. CSI has the potential to achieve cm-level positioning accuracy with a single reference point only. In this study, the authors survey CSI fingerprinting-based indoor positioning and mobility tracking systems. The process of fingerprinting that includes site surveying and signal preprocessing is discussed in detail. They determine the potential challenges of such systems and propose remedies to improve positioning accuracy. In general, spatial diversity, such as multiple-input multiple-output antennas and wireless sensor networks, or frequency diversity (e.g. high subcarrier count, frequency hopping mechanism) are exploited to achieve high positioning resolution. Such IPS can also be enhanced via additional sensors or spatial graphs for motion detection and tracking.

1 Introduction to indoor positioning

Internet-of-Things (IoT) comprises of numerous electronic devices, tags, and sensors embedded in objects or machines. With a massive number of IoT-connected devices, it is inefficient and impractical to broadcast a message to all of them, which consumes large bandwidth and power. Therefore, locating a device and providing it with relevant respective information is the key to the successful applications of IoT in such a vast network.

Three general applications of localisation are navigation, location-based services, and monitoring [1, 2], as shown in Fig. 1. Aside from limiting network broadcasts or messages based on proximity, positioning can be applied for entertainment or emergency. For example, shopping malls can give customers an interactive experience by offering a shopping guide. Disaster and risk management can be improved by providing people with evacuation procedures on a map of the area. It can also assist healthcare professionals in monitoring a patient's vital signs or help in tracking inventory.

Fig. 1 *General applications of localisation*

Localising mobile devices in an outdoor environment typically utilises the Global Positioning System (GPS). This system is the standard for outdoor localisation and provides metre-level accuracy during normal operations. However, standalone GPS is unreliable inside buildings since satellite signals rely on line-of-sight (LOS) and are attenuated by obstructions. Introducing repeaters and directional antennas enable indoor GPS operation with around 10-m accuracy at the expense of additional hardware and storage space [3]. As a result, several other methods for locating mobile devices in an indoor environment are explored. Table 1 summarises various media used in indoor positioning based on [4], which includes benefits and drawbacks of specific technologies for indoor positioning.

Mechanical-based indoor positioning system (IPS) uses inertial navigation system (INS) and inertial measurement units (IMU), such as gyroscopes and accelerometers, to achieve high accuracy. However, such sensors must be embedded onto the device and require filtering methods since they are sensitive to drift and

Table 1 Various media used in indoor positioning based on a survey [4]

Medium	Examples	Advantages	Disadvantages
mechanical	INS, IMU	high accuracy, high MTBF, high energy efficiency	invasive, requires filtering
acoustic	Ultrasonic, sonar	cheap, negligible power	short range, synchronisation
magnetic	Magnetometer	high accuracy, no FCC regulation	sensitive to conductive/ferromagnetic materials
optical	Infrared, Camera	cheap, negligible reflection, not sensitive to multipath	LOS only, short range, privacy concern
RF	WiFi	infrastructure support	LOS only if RSSI
	Bluetooth	ubiquitous, low power	short range
	Zigbee	low power	prone to interference, coordination issues
	UWB	high object resolution	prone to interference
	RFID	high data rate, low energy	low precision, requires multiple tags
	LIDAR	3D visualisation	high memory usage

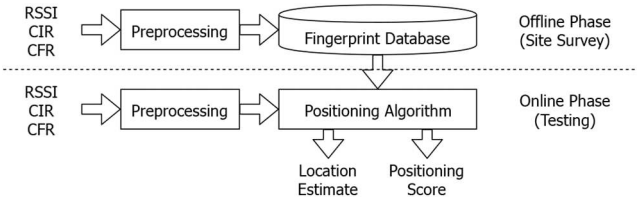

Fig. 2 *Overview of fingerprinting-based IPS*

cumulative error. For instance, a system called Wearable Indoor Localisation Approach uses gyroscopes or magnetometers placed on the waist of the person to count the number of steps and to estimate the length of each step [5]. After testing at different levels of moving speed, the distance estimation error is around 0.5 to 1 m. Imperfect step counting primarily causes this significant error.

Acoustic devices such as ultrasonic and sonar sensors are only used for short-range applications and therefore necessitates high deployment cost and synchronisation procedures if scaled. Systems that use magnetic-field sensors offer high accuracy positioning and are not subject to any regulation from Federal Communications Commission (FCC). The problem lies, however, in the sensors' sensitivity to conductive and ferromagnetic materials. Infrared, LEDs and cameras are examples of optical-based IPS. They use standard transducers, have a minimal reflection, and are not affected by multipath. However, they require LOS and are best only for short-range conditions. Furthermore, camera-based IPS is not conducive for high-privacy situations.

Radio frequency (RF) is one of the conventional media for indoor positioning, mostly because of the ubiquitous low-power sensors. Some popular RF technologies are WiFi, Bluetooth, Zigbee, Ultra-wideband (UWB), radio frequency identification (RFID), and LIDAR. Compared to other media, RF is better because of the support of the infrastructure, typically with more extended range, and the capacity to operate in non-line-of-sight (NLOS) environments.

RF-based systems can be divided into different categories. They can be either active or passive systems [1, 4, 6]. Active IPS also referred to as device-based or tagged IPS consists of engagement between the access point (AP) and the mobile units (MUs) to perform localisation. MU is equipped with a communication interface and is aware of the positioning. If a person is being tracked using active IPS, the person must be carrying an electronic device. On the other hand, passive IPS does not rely on any MU and are hence called device-free or untagged IPS.

RF-based IPS can be further categorised as range-based or range-free [4, 6]. Range-based systems use geometric mapping techniques such as trilateration, triangulation, and multilateration to localise the target object's position. They rely on estimating the distance or the heading from measured parameters like received signal strength indicator (RSSI), time of arrival (ToA), time difference of arrival (TDoA), round-trip time, and angle of arrival (AoA). These techniques require multiple APs to calculate the MU's position and are sensitive to multipath effect [6].

Range-free systems employ fingerprinting to determine an object's location [4]. Each location is represented by a unique channel fingerprint. In fingerprinting methods, IPS extracts features from measured parameters, namely RSSI [7, 8] and channel state information (CSI) [6]. Fingerprints are generated by preprocessing these measured parameters and then they are stored into a database. During the testing phase, a newly acquired fingerprint is compared against the database using a positioning algorithm to estimate the location.

Compared to RSSI fingerprinting, CSI fingerprinting is more preferred since it can operate with only a single AP in both LOS and NLOS environments. It can achieve high positioning resolution up to cm-level and can also be easily supported by existing infrastructure since quite a lot of RF systems are orthogonal frequency division multiplexing (OFDM)-based. Because of this, we study fingerprinting systems which use RF devices to generate CSI unlike in [4], which covers other systems such as mechanical, acoustic, magnetic and optical, as well.

In this paper, we survey recent works relating to CSI fingerprinting-based IPSs in Section 2, as well as mobility tracking systems in Section 4. We demonstrate the basics of the fingerprinting method including channel frequency response (CFR) phase compensation and CFR quality sifting to improve the performance of localisation algorithms such as time-reversal resonating strength (TRRS) and support vector machines (SVMs) in Section 3. Experiments included in this paper highlight TRRS, which is an algorithm that can achieve high positioning and tracking accuracy at the centimetre-level. We then elaborate on potential challenges of these systems, such as dealing with environmental dynamics and site surveying across temporal and spatial domains in Section 5. Lastly, we highlight the importance of this survey and summarise this paper in Section 6.

2 IPS based on CSI fingerprinting

Fig. 2 shows the process of fingerprinting-based IPS. This method has two phases: offline and online. In the offline period, the training data (i.e. fingerprints) are collected via a site survey of the indoor environment. An AP maintains a database of pre-recorded location fingerprints. A location fingerprint is a set of features that can uniquely characterise a position based on the wireless channel condition. In the online phase, the testing data is collected in real-time. To perform localisation, the AP queries the target MU of unknown location and acquires a new fingerprint. It compares the new fingerprint to previously-stored fingerprints in the database using similarity measurement, statistical or machine learning methods to identify the best match as the location of the MU.

Fingerprinting systems utilise wireless measurements such as RSSI and CSI. RSSI is considered as a MAC layer feature, while CSI is a PHY layer feature [6]. RSSI is the combination of all the signals, that travelled across multiple paths, arriving at the receiver. Since all the signals are aggregated, RSSI cannot discriminate the constructive and destructive phase superpositions [6]. RSSI values may even vary up to 10 dB in a time frame of 5 min as environmental changes affect the signal reflection and attenuation [9]. Unlike RSSI that is dependent on LOS, CSI can easily characterise multipath effects in the NLOS environment and can describe a finer-grained channel response. In a multipath-rich environment, scatterers can act as virtual antennas to enable additional degrees of freedom [10].

CSI has two types, namely, channel impulse response (CIR) and channel frequency response (CFR). CIR is a time-domain representation of the complex channel. It describes the magnitude and phase of the channel in time bins, while CFR is its frequency-domain counterpart that depicts the complex channel in frequency subcarriers. An impulse signal is required to generate CIR, while CFR can be easily extracted over devices that utilise OFDM [6]. CIR is also more prone to error due to poor synchronisation [6]. For CFR, phase compensation methods mitigate synchronisation issues.

Prior to positioning, raw RSSI and CSI measurements may undergo preprocessing, such as denoising and feature extraction methods [11]. Raw RSSI readings taken from several APs are preprocessed to extract statistical features (e.g. mean, standard deviation and median) as the fingerprints [12] or to generate radio maps for clustering [9]. As for CFRs, a fingerprint signature can be generated by subtracting the average CFR amplitude and phase from the raw CFR vector [13] or by retaining only the most stable set of subcarriers [14], considering that each subcarrier fades differently. Due to synchronisation issues, sanitising raw CFRs requires estimation of the phase's slope and offset [15, 16], while mitigating non-phase-coherent CIRs needs estimation of non-overlapping multipath components in the time domain [17].

Fingerprinting-based IPS makes use of similarity measurement techniques, as well as statistical and machine learning methods for localisation. Some of these techniques are log-likelihood distance metric [15, 17], Bayes' theorem [13], correlation clustering [9], hidden naive Bayes classifier [18], TRRS [16, 19, 20], *k*-nearest neighbours algorithm (kNN) [12, 13], SVM [14], and linear discriminant analysis (LDA) [21]. Other systems also utilise deep learning algorithms such as an artificial neural network (ANN)

Table 2 Recent works on fingerprinting-based IPS using CSI

Ref.	IPS type	Hardware	CSI type	Frequency band (bandwidth)	MIMO?	Techniques	N/LOS?	Positioning accuracy, m
[19]	active	USRP N210	CIR	5.40 GHz (125 MHz)	no	TRRS	N/LOS	0.10
[16]	active	USRP N210	CFR	5.40 GHz (1 GHz)	no	TRRS	N/LOS	0.05
[20]	active	USRP N210	CFR	5.24 GHz (321 MHz)	yes (3 × 3)	TRRS	N/LOS	0.01–0.02
[13]	active	Intel 5300	CFR	IEEE 802.11n	yes (3 × 3)	kNN, Bayes	LOS	1.5–2
[15]	active	Intel 5300	CFR	IEEE 802.11n	no	Log likelihood	N/LOS	1–2
[23]	active	Intel 5300	CFR	IEEE 802.11n	yes (3 × 3)	DNN, RBF	N/LOS	1–2
[17]	active	UWB DW100	CIR	6.5 GHz (900 MHz)	yes (6 × 1)	Log likelihood	N/LOS	0.20–0.45
[14]	passive	Intel 5300	CFR	IEEE 802.11n	yes (3 × 3)	SVM	LOS	0.75
[21]	passive	Intel 5300	CFR	IEEE 802.11n	yes (3 × 3)	LDA	LOS	1–2
[18]	passive	Intel 5300	CFR	IEEE 802.11n	yes (2 × 2)	HNB	LOS	1–2

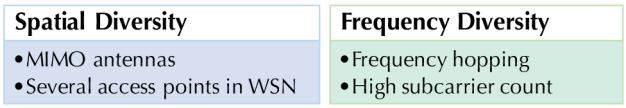

Fig. 3 *Techniques for increasing fingerprint length*

[22], deep neural network (DNN) [23], and deep belief network [24].

In RSSI-based fingerprinting, measurements taken from several APs in a wireless sensor network (WSN) are acquired to position a device. For instance, a system with three APs called RADAR applies nearest neighbours algorithm to find the best match fingerprint with a positioning error of around 2–3 m [12]. Also, a device-free system uses RSSI from multiple anchor points to generate the location fingerprints [25]. Positioning can be performed using classification and radio tomographic imaging methods. With a varying number of anchor points (from 8 to 24), such a system can position with an estimation error of 1.5 to 3 m [25]. Another RSSI-fingerprinting system called Hive5 makes use of a single AP built with directional antennas in a semispherical radiation pattern [22]. ANN is used to localise an acquired RSSI fingerprint with an accuracy of around 1 m. Although this system uses only one AP, it has a relatively high positioning error and it is customised and bulky, which makes commercial implementation impractical.

Table 2 summarises recent CSI fingerprinting-based systems for positioning, considering both active and passive IPS in either LOS or NLOS situations. Positioning accuracy in this table refers to the distance error with respect to a reference point or step size between discrete positions in space. The input features for these techniques are CSI fingerprints of the known locations. Unlike most RSSI-based systems, these active CSI-based IPS only use one AP and achieve low positioning error at cm level.

Most of the systems required database maintenance and did not use a map, floor plan or any additional sensors to improve the positioning performance. The SALMA system [17] incorporated a floor plan of the room including mapping of large obstructions such as chairs, tables, and cabinets and used distance ranging to select a subset of the database as candidate locations. The floor plan assisted in creating a theoretical location fingerprint, making the system calibration-free. However, this system made use of high bandwidth customised equipment to generate signal impulses. For example, TRIPS used exclusive radio system prototypes to create CIRs [16, 19], and SALMA employed a UWB transceiver DW1000 with self-made antennas [17].

Some IPS exploited spatial diversity to increase the number of features in a fingerprint [13, 14, 17, 18, 20, 21, 23]. Utilising more antennas or transmitter–receiver (TX–RX) links can extend CSI fingerprint length. Most IPS gathered CFR samples with 30 subcarriers from multiple antennas. Then, the AP concatenated CSI data from all the antennas to generate the complete fingerprint. On the other hand, the SALMA system followed the IEEE 802.15.4-2015 standard and employed UWB technology to acquire CIR samples up to six antennas [17]. Since the system operated in multiple-input multiple-output (MIMO), there were up to nine links in total. Using more links would lead to CFR fingerprints of larger bandwidth.

Most fingerprinting-based IPS used IEEE 802.11n since off-the-shelf devices support this standard [13, 14, 21, 23]. The Intel WiFi Link (IWL) 5300 network interface card (NIC) operates in either 2.4 or 5.0 GHz frequency band with 20 or 40 MHz channel bandwidth. It supports the use of MIMO antennas [26]. This NIC has been widely deployed in computers to extract CSI features by using a CSI tool in Ubuntu Linux [27]. The recorded CSI per single antenna contains 30 subcarriers. With a MIMO capability of up to three antennas per AP, the collected CFR fingerprint can have up to 90 subcarriers. Because OFDM devices can easily extract samples even with limited channel bandwidth, CFR has been more preferred than CIR for fingerprinting.

Aside from spatial diversity, increasing the length (bandwidth) of the fingerprint can also be accomplished by using frequency diversity [16, 20]. Chen's prototype had 128 subcarriers for each channel [20], which was more than other related systems. Using more subcarriers would provide more information for the fingerprint. Another method for frequency diversity is to use multiple fixed-width channels, where each channel contains 48 subcarriers [16]. In this technique, AP and MU transmit packets one channel at a time using the frequency hopping mechanism, and the effective bandwidth can be increased up to 1 GHz. Fig. 3 summarises the spatial and frequency diversity techniques.

Positioning error is usually in the metre-level range except for some systems employing high bandwidths. Centimetre-level accuracy in NLOS was achieved by CFR fingerprinting using high effective bandwidths [16, 20] or by CIR fingerprinting using impulse signals [17, 19]. Wider bandwidth means richer fingerprint information; richer fingerprint information means lower positioning error.

Other than assessing positioning accuracy, it is vital to investigate how long the validity of the fingerprint database would last. Only some research works evaluated temporal stationarity: one day for TRIPS and SALMA [17, 19], two days for PinLoc [15] and four days for Chen's MIMO system [20]. Although the PinLoc system worked after seven months, the system only had 70% localisation accuracy over a few test spots and has a positioning error of 1–2 m.

In terms of hardware, all IPS listed in Table 2 utilised bulky equipment instead of portable devices. In [16, 19, 20], each transceiver prototype was equipped with a software-defined radio (SDR) and a laptop. Each prototype was customised to operate with the desired frequency band and effective bandwidth. For systems that utilise IEEE 802.11n, laptop computers are used as the target MUs and are connected to off-the-shelf wireless APs. Apart from laptops and APs compatible with IEEE 802.11n, the MaLDIP system even included a dedicated server to process CSI collected from multiple devices for passive positioning [14]. However, in the UWB-based SALMA IPS, the target devices are small battery-powered tags with omni-directional antennas. At the same time, the anchor point is a UWB radio device with customised antennas linked to a dedicated laptop [17]. Although the tags are small, they are not yet integrated into typical hand-held devices.

3 Experiments on CSI fingerprinting-based IPS

In this paper, we also explain the fundamental methods for indoor positioning, as shown in Fig. 4. Our method starts with the

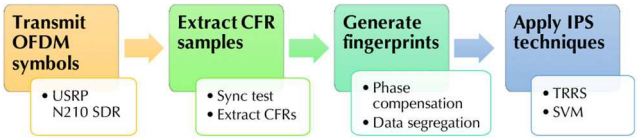

Fig. 4 *Flowchart for CSI-based indoor positioning*

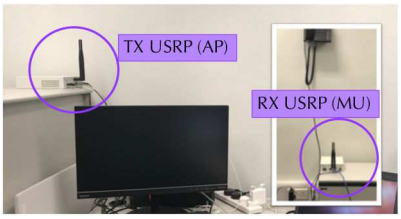

Fig. 5 *Experimental setup of the IPS consisting of two sets of SDR devices and computers*

Table 3 Information about fingerprint datasets

	Dataset A	Dataset B
amplifier gain	25 dB	18–22 dB
# of collection days	2 days	3 days
# of periods per day	11 (day 1)	6 (day 1)
	2 (day 2)	5 (day 2)
		3 (day 3)
total # of fingerprints	520	560
application	fingerprinting	channel quality sifting
used in sections:	3.2, 3.4, and 3.5	3.6 and 3.7

transmission of OFDM symbols, including synchronisation symbols via SDR devices. Raw CFR samples were extracted from the SDR log data files and were phase-compensated before storing into corresponding training or testing datasets. Once the datasets were generated, we applied positioning techniques and investigated their positioning accuracy.

3.1 Experimental setup

Fig. 5 shows the actual experimental setup of our IPS with a transmitter (TX) and a receiver (RX) placed in a typical office environment. Similar to previous works [28, 29], both TX and RX consisted of a USRP N210 SDR device with two 6 dBi antennas and a laptop computer installed with GNU Radio Companion set to 12.5 MHz sampling rate. In this setup, the TX–RX distance was ∼2.5 m. For each collection period, TX was fixed while RX was moved over four locations that are 20 cm apart on top of a flat surface. Each collection period was separated by roughly 15 min.

We collected CSI from at most 30 channels, starting from 3.16 to 3.45 GHz with a 10-MHz increment, per period per location. Concatenation of these channels makes up one sample, which is regarded as a CFR fingerprint. We generated ten fingerprints per period per location; consecutive fingerprints were ∼2 ms apart. Because of the close time separation, data from the same period and location have a high correlation. Since range-free IPS relies on-site survey, we prepared two datasets for both offline and online phases as listed in Table 3.

Dataset A was used to demonstrate the fingerprint preprocessing and positioning performance under varying environmental conditions. In specific periods, we varied the environmental factors such as door opening or closing and obstructed LOS. On the other hand, dataset B contains fingerprints that are utilised to demonstrate the effect of poor channel quality on positioning performance, and the improvement that could be brought upon by using channel quality sifting. To illustrate the effects of poor hardware, we set the gains to lower values ranging from 18 to 22 dB for each period. Unlike dataset A, there is no intentional change in environmental factors.

In this work, we focused on CFRs, which is a type of CSI that can be easily retrieved from an OFDM-enabled AP. We represent CFRs as a vector of complex numbers as shown in (1) [16]. $\hat{H}_{u_k}$ is one complex-valued subcarrier, where u_k is the index of that subcarrier. k has values from one to K, where K is the total number of subcarriers

$$\hat{\boldsymbol{H}} = [\hat{H}_{u_1}, \hat{H}_{u_2}, \ldots, \hat{H}_{u_K}]^{\mathrm{T}} \tag{1}$$

In IEEE 802.11n, the total number of subcarriers is 56, where 52 are data subcarriers, and 4 are pilot subcarriers [30]. Some IPS that operate on IEEE 802.11n utilise IWL 5300 NIC [13, 14, 18, 21, 23]. Although these systems follow IEEE 802.11n, CSI extraction tool from [27, 31] provides only 30 subcarrier groups ($K = 30$), around one group per two subcarriers. As for IEEE 802.11a, the total number of subcarriers is 52, where 48 are data, and 4 are pilot [32]. IPS that followed IEEE 802.11a OFDM format typically use USRP N210 devices which can be configured to extract CSI with $K = 52$ subcarriers [16, 20, 28, 29]. In this paper, we used $K = 52$ similar to the IPS that follow IEEE 802.11a.

3.2 Fingerprint preprocessing using phase compensation

Several wireless sensing applications exploit both CSI magnitude and phase shifts [11]. For instance, changes in CIR amplitudes can be applied to various human activity detections and recognitions. Furthermore, CFR phase shifts caused by spatial links and frequency changes can be exploited to determine delays and directions of signal transmission, which are suitable for positioning and tracking scenarios. However, CSI phase suffers from synchronisation errors such as frequency and timing offsets [16, 33].

Several noise reduction strategies, such as linear regression and phase offset estimations [11], can be employed to remove phase offsets and outliers in CSI. One technique for compensating the phase shifts caused by synchronisation errors was presented in [16]. Channel frequency offset, sampling frequency offset, and symbol timing offset are approximated from adjacent long training preamble symbols that follow IEEE 802.11 frame standard using OFDM transmission. Since our system follows a similar method based on OFDM, we applied the same phase preprocessing.

Fig. 6 illustrates the fingerprint preprocessing applied to two different channels based on the phase compensation procedure in [16]. CFRs of channel A were collected at 3.17 GHz, while those of channel B were acquired at 3.28 GHz. Before sanitisation, CFRs exhibit linear phase whose values vary greatly among the 20 raw samples. After sanitisation, 20 CFRs are reduced to 10 CFRs to remove synchronisation errors. The sanitised samples have relatively flat phase responses, but the phase may still vary among samples. Before concatenation, CFRs that were correlated (i.e. greater than or equal to a correlation coefficient of $\tau = 0.90$) are retained and averaged. The number of retained CFRs after this sifting procedure may be less than ten but must be at least two to allow averaging. All the 10-MHz channels individually underwent the three processes and then concatenated to form the final complex fingerprint. With this preprocessing method, we can generate more stable CFRs and utilise several channels for a location fingerprint with richer information.

Fig. 7 shows two 300-MHz fingerprint samples from two different locations. Each fingerprint consists of 30 phase-compensated CFRs, where each CFR is a 52-subcarrier vector of complex values. The two fingerprint samples are visually distinguishable despite having the same set of 30 channels from 3.16 to 3.50 GHz.

3.3 TRRS-based positioning

Among the positioning techniques in Table 2, TRRS is the best one to achieve centimetre-level accuracy using CFR fingerprints. TRRS $\gamma[\hat{\boldsymbol{H}}, \hat{\boldsymbol{H}}']$ computes the cosine similarity between two fingerprints $\hat{\boldsymbol{H}}$ and $\hat{\boldsymbol{H}}'$ as shown in (2) [16]. $\hat{\boldsymbol{H}}$ is the fingerprint recorded from a known location, while $\hat{\boldsymbol{H}}'$ is the fingerprint from an unknown position. $\langle \boldsymbol{x}, \boldsymbol{y} \rangle$ is the inner product between the two complex vectors $\boldsymbol{x}$ and $\boldsymbol{y}$, which is expressed as $\boldsymbol{x}^{\dagger}\boldsymbol{y}$, where $(\cdot)^{\dagger}$ is

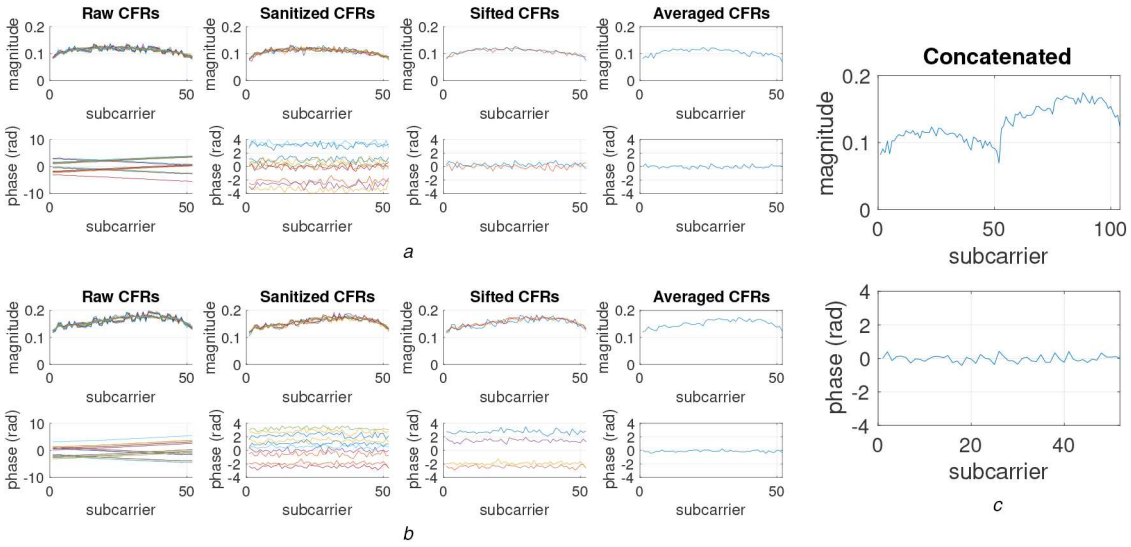

Fig. 6 *Fingerprint preprocessing includes per-channel phase compensation procedure of complex CFRs (Sanitisation, Sifting, and Averaging) and Concatenation of averaged CFRs*

(a) Phase compensation of complex CFR samples from channel A, ***(b)*** Phase compensation of complex CFR samples from channel B, ***(c)*** Concatenation of averaged CFRs from channels A and B

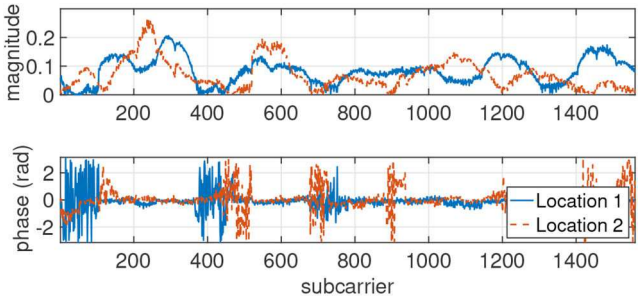

Fig. 7 *Complex fingerprints with 300-MHz effective bandwidth from two locations that are 20-cm apart*

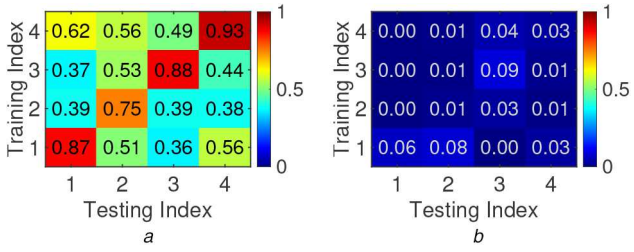

Fig. 8 *Positioning scores where training and testing data are approximately 15 min apart*

(a) With phase compensation, ***(b)*** No phase compensation

the Hermitian operator. Two fingerprints are highly correlated if the value of TRRS is close to 1, while they are not correlated if the value is 0

$$\gamma[\hat{\boldsymbol{H}}, \hat{\boldsymbol{H}}'] = \frac{\left|\sum_{k=1}^{K} \hat{H}_{u_k} \hat{H}'_{u_k}\right|^2}{\langle \hat{\boldsymbol{H}}, \hat{\boldsymbol{H}} \rangle \langle \hat{\boldsymbol{H}}', \hat{\boldsymbol{H}}' \rangle} \tag{2}$$

In TRRS-based IPS, a testing fingerprint $\hat{\boldsymbol{H}}[l']$ is compared against each data in a database, which is comprised of training fingerprints from several known positions or locations. To determine the location estimate after TRRS calculations, we find the training fingerprint $\hat{\boldsymbol{H}}[l]$ that yields the highest TRRS similarity with the testing fingerprint and return the known location l of the said training fingerprint as shown in (3) and (4) [16]. $\hat{l}'$ is the estimated location of l'; Γ is the localisation threshold, that is a tunable parameter to adjust localisation sensitivity. If the TRRS value is less than Γ, no estimate (a value of 0) is returned signifying a failed localisation. In this paper, $\Gamma = 0$ to ensure that an estimate is always returned.

$$l^{\star} = \underset{l=1,2,\ldots,L}{\arg\max}\ \gamma[\hat{\boldsymbol{H}}[l], \hat{\boldsymbol{H}}[l']] \tag{3}$$

$$\hat{l}' = \begin{cases} l^{\star}, & \text{if } \gamma[\hat{\boldsymbol{H}}[l], \hat{\boldsymbol{H}}[l']] \geq \Gamma \\ 0, & \text{otherwise} \end{cases} \tag{4}$$

Although TRRS can achieve cm-level positioning, a downside is that it is sensitive to temporal and dynamic variations. The training database can be updated at regular intervals such that each known location can now be represented as a historical data of fingerprints. Thus, we adopted the following changes in the TRRS algorithm to allow multiple training fingerprints per location [34]:

i. *Continuous fingerprint appending (CFA):* We find the best location estimate given training fingerprints collected across several positions and time stamps.
ii. *Fingerprint averaging (FA):* Each location is represented by the average of all the fingerprints collected at different times from the same location. We find the estimate by comparing the testing fingerprint against the averaged fingerprints.
iii. *Weighted fingerprint averaging (WFA):* Similar to FA except that more weight is given to more recent fingerprints.

3.4 Positioning performance of TRRS on fingerprints with or without phase compensation

Fig. 8 shows the TRRS matrices derived from 300-MHz fingerprints with and without phase compensation.

Each TRRS matrix element contains the positioning score between a single training fingerprint and a single testing fingerprint.

We define the positioning score for TRRS as the similarity measure between two fingerprints based on (2). TRRS scores range from 0.0 to 1.0, as shown in the colour bar. Each column displays the scores of comparing a testing fingerprint against four training fingerprints. A high TRRS score means the corresponding fingerprints are correlated. Ideally, a TRRS matrix should have 1.0 for diagonal elements and 0.0 for off-diagonal elements so that each testing fingerprint is accurately positioned. Realistically, a TRRS matrix shows correct positioning when the highest TRRS score for each column is the diagonal element.

The two TRRS matrices reveal the importance of phase compensation in complex fingerprints. Training and testing fingerprints for these TRRS matrices are collected ~15 min apart

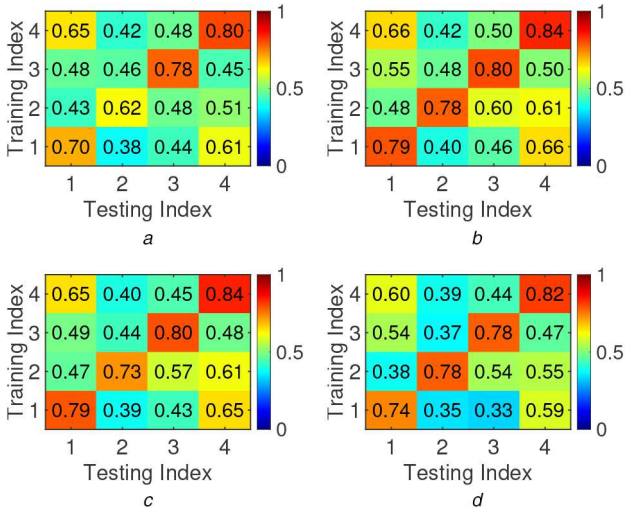

Fig. 9 *Positioning scores of various TRRS techniques where training and testing data are one day apart*
(a) TRRS, ***(b)*** TRRS with CFA, ***(c)*** TRRS with FA, ***(d)*** TRRS with WFA

Table 4 Positioning accuracy under temporal conditions

Bandwidth, MHz	TRRS w/ CFA	TRRS w/ FA	TRRS w/ WFA
300	1.00	1.00	1.00
200	1.00	1.00	1.00
100	0.75	0.75	0.74
40	0.71	0.55	0.68

Table 5 Positioning accuracy under dynamic conditions

Bandwidth, MHz	TRRS w/ CFA	TRRS w/ FA	TRRS w/ WFA
300	1.00	1.00	1.00
200	0.88	0.88	0.99
100	0.86	0.83	0.74
40	0.49	0.50	0.50

when there are no obvious changes in the environment. In Fig. 8*a*, all testing data are correctly positioned. However, in Fig. 8*b*, positioning fails, and even same-location fingerprints have close to zero scores.

Fig. 9 displays TRRS matrices when we evaluated the positions of 300-MHz testing fingerprints against a fingerprint database. For TRRS w/ CFA, FA and WFA techniques, a database consisting of 280 fingerprints in dataset A was used. For the original TRRS algorithm, only four training fingerprints were utilised, as shown in Fig. 9*a*. The four testing fingerprints were acquired one day after collecting the training fingerprints. Since the highest value per column is the diagonal element, using any of the three enhanced TRRS strategies results in correct localisation after one day. On the other hand, an off-diagonal value for the original TRRS is close to the diagonal value, as shown in the first column of Fig. 9*a*. This indicates that there is a minimal margin of error between correct and incorrect positioning. Among the four TRRS techniques, TRRS w/ CFA has the highest average diagonal value of 0.8008, while the original TRRS has the lowest average diagonal value of 0.7248.

Performance difference among the strategies depends on the environments and effective bandwidths of the fingerprints. For instance, Tables 4 and 5 summarise the positioning accuracies of the TRRS techniques when the bandwidths are varied and when there are temporal or dynamic environmental variations. We define accuracy as the ratio of the number of correctly positioned testing fingerprints over the total number of testing data.

In Table 4, the training and testing databases were comprised of 280 fingerprints from day 1 and 80 fingerprints from day 2 of dataset A, respectively. These fingerprints did not consider intentional changes in the indoor office setup. In almost all the high-bandwidth scenarios (e.g. 200 MHz, 300 MHz), all the 80 testing fingerprints results in perfect localisation. On the other hand, positioning accuracy decreases as the effective bandwidth decreases. Given that positions are 20 cm apart, this high-bandwidth TRRS-based positioning system can, therefore, localise at cm-level.

Although all techniques showed similar positioning accuracy under temporal conditions, CFA may be more appropriate in a longer time frame. It is because both FA and WFA are averaging techniques, which there are losses in the stored information. Fingerprints from the same position may have less TRRS similarity if there are changes in the environment. However, TRRS w/ CFA requires more storage space [34] and slightly longer processing time [28] than the other two TRRS remedies.

In Table 5, the training and testing databases were comprised of 280 and 160 fingerprints, respectively, from day 1 of dataset A. The training fingerprints were baseline data when there were no changes in the environment (i.e. the door is closed, no obstacle between TX and RX). However, the testing data included environmental variations such as door opening and obstructed LOS. This table exhibits how the positioning accuracy may be affected by environment dynamics. At 300-MHz bandwidth, we can expect perfect positioning accuracy in all TRRS techniques. At other bandwidths, the performance of all three strategies are good, but TRRS w/ CFA exhibits slightly better results. Since TRRS w/ CFA does not employ averaging, the database retains more variance, which is essential for dynamic scenarios. With respect to this result, we apply TRRS w/ CFA in succeeding experiments.

3.5 Positioning performance of TRRS and SVM under various environmental conditions

Another positioning system is based on multi-class SVMs. SVM is a common solution to classification problems by evaluating the dot product between vectors and is an algorithm that works well even if the number of samples is in the same order as the number of features [35]. SVM often provides high accuracy, fast classification speed and capability of handling irrelevant features unlike kNN and Bayesian techniques [35]. By using SVM, we can build a classification model, which cannot be done with similarity measurement techniques like TRRS.

In binary classification, we compute the score of a typical linear SVM based on (5) and then apply a threshold to convert the score into binary 1 or 0 [36]. In this equation, $\hat{\boldsymbol{H}}$ is the fingerprint being tested while $\hat{\boldsymbol{H}}_k$ is one of the support vector fingerprints determined after training the SVM model. y_k is the target value of either +1 or −1 pertaining to the class of the kth element in the support vector set, α_k is the kth Lagrangian multiplier, and b is the bias parameter

$$f(\boldsymbol{x}) = \sum_{k \in S} \alpha_k y_k \hat{\boldsymbol{H}}_k \cdot \hat{\boldsymbol{H}} + b \tag{5}$$

For positioning problems that consider more than two locations, we employ multi-class SVM [28]. Different kernel functions can be utilised instead of the standard linear function. In this work, we applied vector normalisation such that SVM-based IPS also considered cosine similarity like TRRS as in (6) [29]

$$f(\boldsymbol{x}) = \sum_{k \in S} \alpha_k y_k \frac{\hat{\boldsymbol{H}}_k}{\left|\hat{\boldsymbol{H}}_k\right|} \cdot \frac{\hat{\boldsymbol{H}}}{\left|\hat{\boldsymbol{H}}\right|} + b \tag{6}$$

In Matlab, we used `fitcecoc` function for training a multi-class SVM model then applied such model to the `predict` function for classifying our testing data. We define the positioning score found in succeeding SVM matrices as the average binary loss across the SVM binary learners, which can be extracted as an output from `predict`.

Fig. 10 shows the TRRS and SVM matrices when we localise 300-MHz testing fingerprints collected 3 h after the training data. The training database consists of 120 fingerprints in dataset A, while the four testing fingerprints were acquired either ∼3 h or 1 day later. For these positioning matrices, we assess TRRS w/ CFA

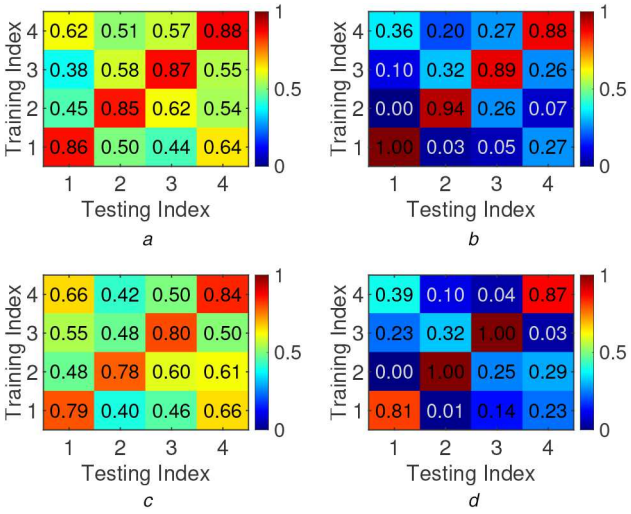

Fig. 10 *In Figs. 10a and 10b, training and testing data are approximately three hours apart. In Figs. 10c and 10d, training and testing data are a day apart*

(a) TRRS w/ CFA (3 h), ***(b)*** Linear SVM (3 h), ***(c)*** TRRS w/ CFA (1 day), ***(d)*** Linear SVM (1 day)

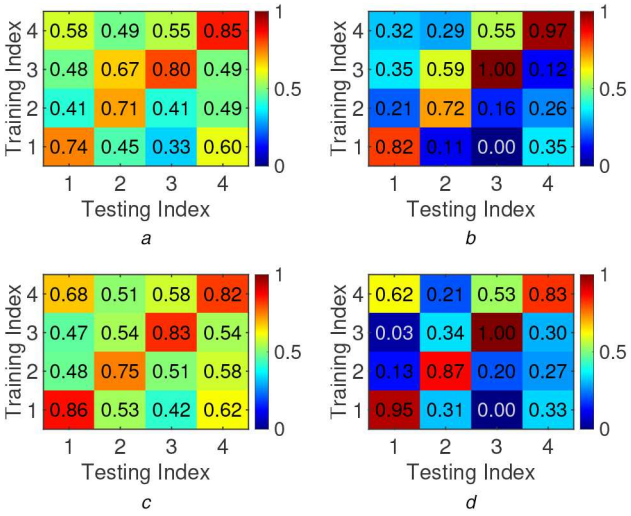

Fig. 11 *Positioning scores of TRRS w/ CFA and Linear SVM wherein the testing data were collected when the environment changed. In Figs. 11a and 11b, an initially closed door was opened. In Figs. 11c and 11d, a large object blocked the LOS between TX and RX*

(a) TRRS w/ CFA (door), ***(b)*** Linear SVM (door), ***(c)*** TRRS w/ CFA (blocked), ***(d)*** Linear SVM (blocked)

Table 6 Positioning accuracy under temporal conditions

Bandwidth, MHz	TRRS w/ CFA	SVM		
		(linear)	(rbf)	(poly3)
300	1.00	1.00	1.00	1.00
200	1.00	1.00	1.00	0.94
100	0.75	0.80	0.69	0.25
40	0.71	0.81	0.83	0.49

Table 7 Positioning accuracy under dynamic conditions

Bandwidth, MHz	TRRS w/ CFA	SVM		
		(linear)	(rbf)	(poly3)
300	1.00	1.00	1.00	1.00
200	0.88	0.88	0.99	0.96
100	0.86	0.88	0.83	0.25
40	0.49	0.54	0.48	0.40

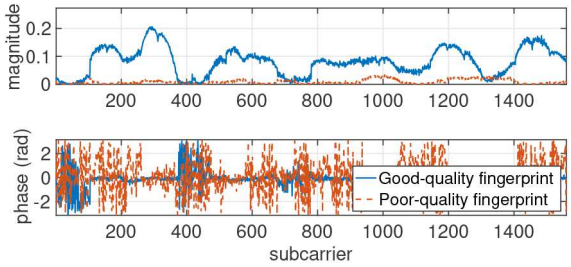

Fig. 12 *Good- and poor-quality fingerprints*

and multi-class linear SVM. For better comparison to TRRS, we scale the SVM scores to a range between 0 and 1. Looking at the TRRS and SVM matrices in a column-wise manner, each testing fingerprint is correctly positioned. Both TRRS w/ CFA and linear SVM achieve correct localisation of high-bandwidth fingerprints under temporal conditions [28].

Fig. 11 displays the TRRS and SVM matrices in which we localise 300-MHz testing fingerprints collected after some noticeable changes in the environment. The training database consists of 280 fingerprints in dataset A. In Figs. 11*a* and *b*, the four testing fingerprints were collected when the door was open. In Figs. 11*c* and *d*, the four testing fingerprints were collected when an obstacle blocked the LOS. Although some off-diagonal elements have higher positioning scores, both TRRS w/ CFA and multi-class linear SVM show correct localisation even under dynamic scenarios.

Tables 6 and 7 list positioning performance of TRRS w/ CFA and various SVM kernels under temporal and dynamic conditions. Results include linear, radial basis function (Gaussian), and third order polynomial functions as kernels to multi-class SVM. The training database contains 280 location fingerprints. The testing datasets for temporal and dynamic conditions include 80 and 160 fingerprints, respectively. In most cases, linear SVM achieves the best performance compared to TRRS w/ CFA and other SVM systems. Also, linear SVM shows slightly better performance over Gaussian SVM in most cases and is around 6–20% faster in terms of computation time. With high-bandwidth (e.g. 300 MHz), all techniques have close-to-perfect positioning performance [16, 28].

3.6 Channel quality detection and fingerprint sifting

For a fingerprint to be considered good quality, it should consist of several good channels [29]. In a good-quality channel, extracted CFR samples have stable and linear phase after phase compensation. If CFR samples are noisy and have unstable phase after compensation, then the channel is of low quality. Noise, interference or hardware instability are common causes of poor CFR quality [29].

Fig. 12 shows sample fingerprints from dataset B with good- and poor-quality channels. Based on the image, the good fingerprint has relatively higher subcarrier magnitudes and more stable subcarrier phases across the 300-MHz bandwidth. On the other hand, a poor fingerprint contains several noticeably erratic phases.

To understand what good and poor CFR samples are, we assess Matlab-generated histograms using the data for subcarrier magnitudes $|H_{u_k}|$, phases $\measuredangle H_{u_k}$, and inter-subcarrier phase difference $\measuredangle H_{u_k} - \measuredangle H_{u_{k+1}}$, as shown in Fig. 13. Similar to results in [29], the histograms approximate common probability distributions; subcarrier phases can be modelled with one side (positive side) of the distribution as in [28] or with both positive and negative sides as in Fig. 13. We can estimate the probability density functions of the CFR properties from good- and poor-quality fingerprints as shown in Table 8. Parametric functions such as Beta, exponential and *t* location-scale distributions can represent all CFR properties except inter-subcarrier phase difference.

We further quantified the CFR properties of good and poor samples, as listed in Table 9. For each CFR sample, we calculated the statistical properties of subcarrier magnitudes, phases, and phase differences. Signal-to-noise ratio (SNR) is the ratio of the

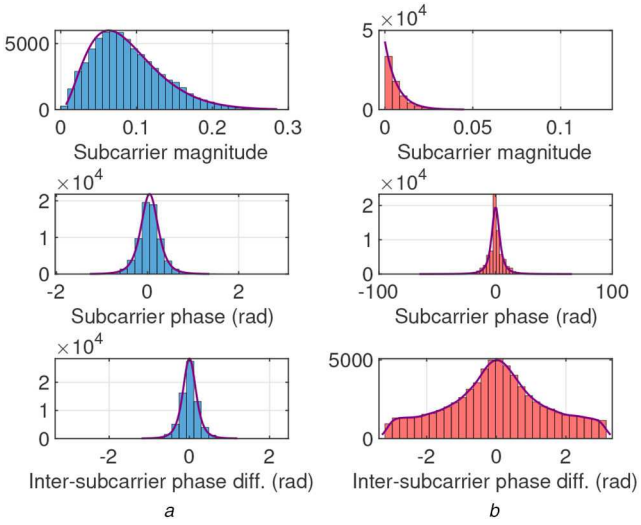

Fig. 13 *Histograms of Dataset B CFRs' subcarrier magnitudes* $|H_{u_k}|$, *subcarrier phases* $\measuredangle H_{u_k}$, *and inter-subcarrier phase differences* $\measuredangle H_{u_k} - \measuredangle H_{u_{k+1}}$ *from good- and poor-quality fingerprints*

(a) CFR samples from good-quality fingerprints, ***(b)*** CFR samples from poor-quality fingerprints

Table 8 Estimated CFR probability distributions using Matlab `fitdist` function on empirical datasets

Property	Good CFR samples		Poor CFR samples	
	Distribution	Parameters	Distribution	Parameters
$\|H_{u_k}\|$	beta	$\alpha = 3.079$, $\beta = 31.810$	exponential	$\mu = 0.00683$
$\measuredangle H_{u_k}$	*t* location-scale	$\mu = 0.043$, $\sigma = 0.194$, $\nu = 3.912$	*t* location-scale	$\mu \simeq 0$, $\sigma = 3.524$, $\nu = 2.030$
$\measuredangle H_{u_k} - \measuredangle H_{u_{k+1}}$	*t* location-scale	$\mu = 0.0016$, $\sigma = 0.169$, $\nu = 3.742$	kernel	normal kernel, $h = 0.155$

Table 9 Quantitative properties of acquired good and poor CFR samples

Property	Good CFRs	Poor CFRs
$\|H_{u_k}\|$ mean	0.0883	0.0068
$\|H_{u_k}\|$ stdev	0.0460	0.0083
$\measuredangle H_{u_k}$ mean	0.0458	0.0715
$\measuredangle H_{u_k}$ stdev	0.2721	6.5211
$\measuredangle H_{u_k} - \measuredangle H_{u_{k+1}}$ mean	0.0011	0.0024
$\measuredangle H_{u_k} - \measuredangle H_{u_{k+1}}$ stdev	0.2400	1.4483
SNR mean	16.7 dB	5.2 dB
SNR min	3.6 dB	N/A
SNR max	22.8 dB	12.9 dB
SNR stdev	15.9 dB	5.2 dB

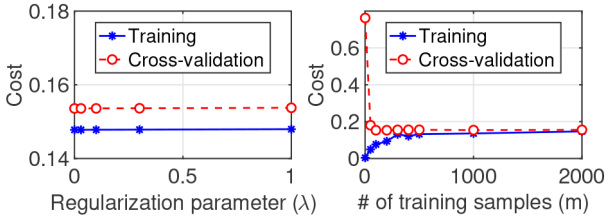

Fig. 14 *Learning curves showing the cost of the logistic regression classifier with 8 statistical features as input vectors at varying regularisation parameter and number of training samples*

signal power to the noise power, where the signal power is shown in (7) [37].

$$P_s = \frac{1}{K}\sum_{k=1}^{K}\left|\hat{H}_{u_k}\right|^2 \tag{7}$$

Compared to CFR samples from poor-quality fingerprints, CFRs from good-quality fingerprints have relatively higher subcarrier magnitudes and lower subcarrier phase variances. Good samples typically have higher SNR. However, there were also cases which poor samples have SNR values close to typical values of good CFRs; such cases were evident in LOS environments [29]. Minimum SNR of good samples can be lower than the mean SNR of poor samples; while minimum SNR of poor CFRs is not available since these cases happened when synchronisation failed (i.e. the signal was too noisy). As a result, SNR itself is not a sufficient measure to determine whether a CFR is of good- or low-quality [29].

As a solution for identifying the channel quality, we devised a binary classifier to distinguish good CFRs (binary 1) from poor CFRs (binary 0) [29, 38]. This classifier used logistic regression model optimised by the gradient descent algorithm. A CFR dataset of 24,000 samples was divided into three: 60% for training the classifier, 20% for cross-validation, an 20% for testing the chosen classifier model. Input data of the classifier can be any of the three:

i. 104 raw features, comprised of both 52 magnitude and 52 phase values from the complex CFR sample;
ii. 8 statistical features, comprised of mean, maximum, minimum, and standard deviation values from both magnitude and phase values of the complex CFR sample;
iii. 60 features, generated by applying principal component analysis (PCA) to the 104 raw features.

Fig. 14 shows the cost function output of the logistic regression classifier at different regularisation values and training sample sizes. According to the figure, varying the regularisation parameter of this classifier does not improve the cost, while utilising 500 or more training samples allows the classifier to converge to its optimal cost value, and further increasing the sample size does not improve the cost. In both graphs, we can see that the logistic regression classifier has low costs. The relationship between the training and cross-validation learning curves indicates whether a chosen model suffered from high variance or high bias [39]. When both training and cross-validation costs are close to each other, we can say that the classifier model is neither overfitting nor underfitting. With respect to this result, we use logistic regression classifier without regularisation and with at least 500 training samples in this paper.

Table 10 shows the performance of our logistic regression classifier at different input features. Various performance metrics, such as accuracy, precision, recall, and F1 score, are shown. All three input features show good results, but a classifier with statistical features as input shows the best performance. With respect to this, we employed statistical features as input to the logistic regression classifier.

This CFR quality classifier can distinguish which channels in the fingerprint is good or poor based on eight statistical features [29]. Good channels are retained in the fingerprint, while poor channels are removed. The number of retained channels depends on the desired fingerprint bandwidth. Sifted channels should be the same across training and testing fingerprints to ensure consistency. In the next subsection, we show that applying fingerprint sifting can improve positioning accuracy in both TRRS and SVM.

3.7 Performance of TRRS and SVM on sifted fingerprints

Table 11 shows the performance of IPSs when channel conditions are less than ideal; that is, channel noise is not negligible. In this table, the training and testing databases were comprised of 440 fingerprints from the first two days and 120 fingerprints from the last day of dataset B, respectively. At 300 MHz bandwidth without

Table 10 Performance of logistic regression classifier at different input features

Metric	Raw features	Statistical features	PCA features
accuracy	0.9340	0.9492	0.9402
precision	0.9191	0.9415	0.9443
recall	0.9117	0.9263	0.8992
F1Score	0.9154	0.9338	0.9212

Table 11 Positioning accuracy when channel conditions were less than ideal

Bandwidth, MHz	TRRS w/ CFA	SVM (linear)
300	1.00	1.00
200	0.93	0.92
100	0.77	0.92
40	0.33	0.20
200 (sifted)	1.00	1.00
100 (sifted)	1.00	1.00
40 (sifted)	0.58	0.68

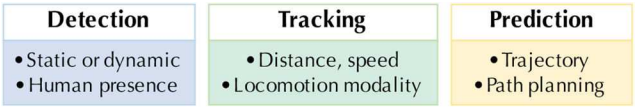

Fig. 15 *Positioning for mobility-related scenarios*

Table 12 Recent works on fingerprinting-based systems for mobility-related scenarios

Ref.	Detect motion?	Estimate distance?	Predict path?	Locomotion modality	Use spatial graph?	Performance
[40]	yes	No	no	none	no	95% (LOS only)
[41]	yes	No	no	stand, walk, sit	no	92–100% (high fs)
[42]	yes	No	no	strenuous human motion	no	up to 90% (high fs)
[43]	no	Yes	no	none	yes	0.05 m/s
[44]	no	Yes	no	none	yes	0.02–0.50 m
[45]	no	Yes	no	none	no	0.36–0.14 m
[46]	no	Yes	yes	none	no	0.57–1.13 m
[47]	no	Yes	no	stand, walk, fall	yes	0.16–0.46 m
[48]	no	Yes	no	stand, walk	no	0.70–0.80 m

fingerprint sifting, both TRRS and SVM techniques achieve perfect accuracy. On the other hand, systems experience inaccurate localisation at low bandwidth scenarios without fingerprint sifting.

By applying our channel quality classifier, the positioning performance is significantly improved. In TRRS w/ CFA, accuracy increases by about 8–73%. In multi-class linear SVM, accuracy improves as high as 238%. Such results are consistent with our previous work [29], which indicate that fingerprint sifting can significantly improve the positioning performance even when the environment is imperfect.

4 Positioning and motion estimation

Mobility tracking systems utilise the positioning algorithms for instantaneous detection and localisation of the target. Thus, the performance of the positioning component is critical to the performance of the mobility tracking system itself.

Applications of positioning system related to mobility-related scenarios are shown in Fig. 15. In motion detection, the system determines whether a target is static or dynamic or whether a person is present in the indoor environment. Another application is tracking the distance and speed of a moving target, as well as the locomotion modality of a person (e.g. sit, stand, walk, and run). Furthermore, mobile tracking can be extended to motion prediction.

Table 12 provides a list of recent fingerprinting-based systems for mobile scenarios, such as various human activities and different moving objects. The performance column in this table indicates the detection percentage for motion detection systems and the approximate estimation error for motion tracking systems. Most mobility-related scenarios focused on motion detection, distance/speed estimation and locomotion modality, instead of trajectory prediction and path planning, which are significant for specific positioning applications such as navigation in emergencies.

All systems operated in both LOS and NLOS indoor environments except the FIMD system [40]. Proposed by the authors of [43, 44, 49] were active indoor positioning; while others [45, 46, 48] were passive systems that relied on multiple coordinated APs to localise the target. Although the motion detection system in [42] was passive or device-free, the setup only required a pair of transmitter and receiver instead of several coordinated APs.

Some of these systems used CSI fingerprinting, specifically CFR [40, 41, 46, 49] and CIR [42–44]. While WiSpeed utilised CSI [47], the system only relied on the CFR amplitude to describe the electromagnetic power of the waveform. Other systems used RSSI vectors produced from multiple APs [45, 48].

Two applications of mobility-related positioning systems are motion detection and motion tracking Fig. 16. For motion detection, the system determines whether the target is moving or not. For instance, FIMD performed passive motion detection using machine learning, particularly, clustering of CFR features into static and dynamic groups [40]. Although FIMD achieves around 95% motion detection rate, this system only operates in LOS scenario. Another system is MoSense, which passively detected human movements such as sitting, standing, and walking based on changes in the channel states [41]. It achieves high detection rate of 92–100% at the expense of high CFR sampling rate (i.e. 100 CFR samples per second). Unlike FIMD and MoSense that required multiple coordinated APs, a motion detection system using only a pair of TX-RX devices can detect taxing human movements (i.e. fast and broad limb movements, kicking etc.) [42]. This device-free

system first detected whether the environment was LOS or NLOS to classify movement vigorousness with up to 90% detection rate. A downside of these three systems is their high sampling requirement.

Motion tracking systems estimate the covered distance or the speed of the moving target with errors typically lie below 1 m. Some systems employ hybridisation to augment the fingerprinting positioning performance and achieve centimetre accuracy. WiBall utilised a spatial graph, IMU sensors, and floor map in addition to CIR fingerprinting [44]. The spatial graph describes the trend of the CSI in the spatial domain and estimates the change in distance. For example, the spatial graph in WiBall shows that there is a spatial resonating decay when the CIR fingerprint similarity is calculated based on the TRRS technique. Such a decaying pattern is identified as Bessel-function-like. Since distance estimation provides no information regarding the bearing and may have successive positioning errors, the IMUs and floor map are incorporated for direction estimation and error correction, respectively.

Other systems also investigated the spatial behaviour of the positioning performance similar to [44]. In [43], a joint Gaussian approximation model can represent the TRRS-based resonating decay of CIRs. In WiSpeed, the spatial decay of the autocorrelation function of the CFR amplitude fingerprint has an oscillation of $\sin(k\nu\tau)/(k\nu\tau)$ [47]. Although the systems that employed spatial graph achieved good performance, they used high sampling rates, e.g. 200 CIR samples per second [44], 100 CIR samples per second [43] and 1500 CFR amplitude samples per second [47]. In addition, two of them used CIR, which required special equipment to generate.

Instantaneous information such as direction (e.g. heading, turning) and displacement (e.g. step length, step count) can describe human mobility [50]. These measurements can be analysed to produce more complex information about human mobility such as trajectory, locomotion modality, and context landmarks (e.g. elevator, stairs, and corridors). Such complex information describes human mobility behaviour, as well as distinguishing locomotion modality [41, 47, 48].

The hardware deployed in these mobility-related systems were similar to that of the CSI fingerprinting-based IPS in Section 2. For instance, a setup typically involves a commercially available wireless AP and a laptop computer as the target device with the CSI tool [27]. Other works had both anchor points and target devices as customised transceiver prototypes, wherein each prototype was a set of laptop and SDR [43, 44]. In systems that employed passive positioning, small sensor nodes can communicate with APs in WSNs using the IEEE 802.15.4 protocol [48] on the 433.1 MHz or 909.1 MHz unlicensed bands [45] to extract RSSI fingerprints.

5 Challenges and future directions

5.1 High bandwidth requirement

As presented in Table 6, various positioning algorithms that utilise high bandwidth fingerprints can accurately discriminate positions that are close together. Hence, centimetre-level localisation is possible with high bandwidth CIR/CFR-based fingerprinting [16, 19]. Higher bandwidth means more information or features to represent a position and therefore, better for pattern recognition.

Fingerprints with large bandwidth can be generated by utilising spatial diversity or frequency diversity. CIR-based fingerprinting can guarantee good positioning performance by using either an omnidirectional antenna or multiple directional antennas [17]. However, this approach required large equipment to generate a good impulse signal. More fingerprint information can also be attained by concatenating CFRs from several TX–RX links, which are from MIMO antenna arrays [20, 23]. These antenna arrays are much smaller and require less additional processing. Since several commercial APs already employ MIMO, incorporating CFRs from multiple links is more practical than implementing bulky equipment. Aside from antenna arrays, we can consider CFRs collected from several collaborative APs in WSN.

In addition to the spatial domain, we can employ frequency diversity techniques such as frequency hopping [16] or higher subcarrier count on a fixed-width channel [20]. In frequency hopping, IPS can collect CFR one channel at a time. This method requires precise synchronisation and handshaking method between the AP and MU [16] and channel access scheme to avoid collisions or interference in contested wireless networks. Since channel switching may take a longer time, it may not be practical for mobile positioning systems that require high CSI sampling rates. We can opt for using higher subcarrier counts on fixed-width channels. For instance, [20] implemented the 40-MHz mode of IEEE 802.11n where there were 114 out of 128 usable subcarriers. This 114 subcarrier count was higher considering that the CSI tool only reported 30 subcarriers in either 20 or 40 MHz mode [27]. Thus, more information about the channel can be recorded.

5.2 Environment noise and dynamics

Environment noise and dynamics significantly affect the quality of CSI fingerprints. As shown in our experiments, mislocalisation often occurred when CSI was extracted from low-quality channels. Noise, interference or hardware instability can cause such poor quality [29]. Other works suggested the use of noise reduction techniques such as Pauta criterion [18], averaging [21], and outlier removal [11]. For IPS that did not utilise sophisticated channel access techniques, only CFRs that can be successfully decoded were stored to ensure CSI quality, and phase compensation procedure only eliminated synchronisation errors [16, 20]. However, in these IPS, there were no discussions on how to determine the CFR quality.

High SNR does not always guarantee the good quality since SNR computations rely on subcarrier amplitudes, while erratic subcarrier phases can as well characterise low quality. Thus, a channel quality detector based on supervised learning can be used to evaluate the channel condition. Fingerprint quality can still be poor even if CFRs were successfully extracted and compensated, as shown in Fig. 12. This quality classifier can be applied to sift out poor channels in real-time or offline and retain only CFRs of good quality [29]. IPS can also apply phase concealment techniques as an alternative to fingerprint sifting, which can be done by replacing poor channels with the average neighbouring channels or with a theoretical model.

Temporal and environmental dynamics such as changes in the scatterers' positions and human movement can alter fingerprint information due to changes in the transmission and reflection paths [51, 52]. Signal strengths are affected by human presence and humidity, as well as dynamic power control in devices [7]. For instance, human activities near the APs can slightly decrease the true positive localisation probability P_{TP} by 1–2%, while the drastic changes in environment like a door opening and closing can reduce P_{TP} by 2–8% for high bandwidth scenarios [20]. Correlation between CFR fingerprints using TRRS can decay from 90 to 70% over four days [20]. When the correlation is severely degraded, and the channel stationarity cannot be met, IPS require database maintenance as often as once a day [34]. IPS should, therefore, be more robust against these changes to avoid frequent update and maintenance. If we can model how CFRs or CIRs evolve over time or space, the frequency of database maintenance can be significantly reduced.

5.3 Site survey and calibration

In site survey, also called wardriving, samples at discrete positions in the areas of interest are collected and labelled accordingly to build the fingerprint database [6, 50]. Such an offline process raises a number of questions: (i) what should be the spatial granularity between positions? and (ii) how to annotate or label samples?

The granularity describes the grid size of the site survey. Smaller grid size means smaller positioning error but more time-consuming site survey. Grids with centimetre resolution required complex setup such as the channel probing table in [16, 19, 20, 44]. This table was used to precisely move a transceiver on desired locations. Wardriving for CSI fingerprinting was typically done in

a 2D environment, as recent works on 3D localisation only focused on RSSI-based ranging [53] and RSSI-based fingerprinting in a WSN [54].

The fingerprint database contains the samples together with the labels or locations. Annotating samples is another challenge. These annotations are necessary for supervised learning algorithms. The PinLoc system labelled CFR packets based on the current position of a robot moving at a constant speed on a predetermined trajectory [15]. Packets falling under one time window were assigned to one spot, which is an area of 1 m^2. Another technique was to collect samples from one reference point at a time on a channel probing table. Because of such deployment need, site survey is time-consuming. Remedies for site survey challenges include maps, user participation, indoor landmarks, and additional sensors [8].

Due to the temporal and environmental changes, fingerprinting-based IPS require database recalibration to guarantee that stored data are relevant. Manual calibration is as tedious as the initial site survey itself. Some techniques to reduce offline site survey involve explicit and implicit crowd-sourcing RSSI data from users, as well as analysing users' unassociated RSSI data to locations [7]. These, however, rely on user participation and therefore, the incentive must be considered.

Some calibration-free solutions rely on theoretical modelling of the spatial domain. For example, the square of the zeroth-order Bessel function of the first kind can approximate TRRS distribution [44]. This function approximates how TRRS values between two CIRs decays and ripples over space, particularly in terms of wavelength. Another estimate of the TRRS between two CIRs could be done based on Joint Gaussian approximation [43]. Furthermore, a spatial graph based on the autocorrelation function of the electromagnetic waves (i.e. CFR amplitude) can be represented as $\sin(k v\tau)/(k v\tau)$ [47]. Since the peaks and valleys in the spatial graphs are related to the wavelength, we can then estimate the distance as well as speed. Another calibration-free strategy theoretically models how the multipath propagation from UWB transceiver given the floor plan and layout of obstacles such as tables, chairs, or cabinets [17]. Such a technique, however, requires high bandwidth CIRs from large UWB-based devices.

5.4 Bulky equipment

Most indoor localisation equipment, including tracked devices, are large and bulky. In CFR-based active positioning systems, tracked devices are either a set of SDR connected to a laptop [16, 19, 20] or a laptop computer equipped with a CSI tool [13, 15, 18, 21, 23]. In [19], the CIR-based system also utilised laptop and SDR. Besides, the SALMA used small battery-powered tags as target devices and extensive customised antenna system as AP [17]. These tags, however, are portable and can eventually be included in small embedded systems. Other CSI-based systems used microcomputers as dedicated target devices for wireless sensing [55, 56]. CSI tools based on different wireless chips such as Intel [27], Atheros [57] and Broadcom [58] are available for a variety of devices, including laptops, embedded devices and smartphones.

Using large or customised equipment to monitor or navigate indoors would not be practical. This calls for transitioning CSI-based positioning into more portable and user-friendly mobile devices, such as smartphones. New smartphone-based systems rely on RSSI instead of CSI for positioning and tracking [52, 59, 60] or on frequency modulated continuous wave to estimate the distance from contours [61]. Using WiFi RSSI data collected for one month, a phone can be tracked using machine learning techniques with performance comparable to CSI-based IPS consisting of a laptop and AP [52].

It is possible, however, to integrate the CSI tool [27] into smartphones. For instance, a desktop computer equipped with IWL 5300 NIC can estimate the AOA from the antenna array of an Android phone with the CSI tool [51]. The Nexmon project enables CSI collection in devices equipped with Broadcom chips, including the latest smartphone models and minicomputers [58]. Another application of the CSI tool on smartphones could be the extrapolation of keystrokes based on CSI fluctuations for security-related attacks [62]. Future works can focus on using CSI on smartphones to warrant portability in positioning and tracking.

5.5 Hybridisation: CSI and other data

Hybrid systems integrate at least two different techniques or media to accomplish better localisation and tracking. CSI data are used for position estimation, while IMU data are for heading estimation [44]. Floor maps improve location estimates in indoor environments [17, 44, 59]. RSSI data can help identify candidate positions from the training database [17]. Herrera *et al*. [59] combined multiple sensing data, namely, RSSI beacons, IMU information, indoor floor plan from OpenStreetMap, and a probability map to achieve a smartphone-based pedestrian tracking system. Since each medium offered different benefits, the combination of two or more media would compensate for the weaknesses of the individual medium. CSI-based fingerprinting can also incorporate RSSI-based ranging to minimise site survey labour, and floor plans can be used to correct localisation errors.

6 Conclusion and future work

In this survey paper, we have provided a comprehensive review of indoor positioning and motion tracking systems. In general, positioning techniques are primarily fingerprinting-based and ranging-based, as shown in Table 13. Unlike ranging techniques that utilise multiple APs, fingerprinting is a range-free technique that employs either RSSI or CSI from a single AP to localise a target. Most survey papers investigated positioning systems that utilise signal strength (e.g. RSSI), time (e.g. ToA) or angle (e.g. AoA) as the measured parameter. These parameters are often sensitive to multipath effects compared to CSI, a PHY layer parameter that can better describe finer-grained channel response in both LOS and NLOS conditions. Survey papers on CSI fingerprinting consider location estimation only but not motion detection nor tracking. As a result, our survey paper focuses on CSI fingerprinting-based positioning and tracking systems for indoor environments.

In addition, we have demonstrated the CSI fingerprinting method, including the benefits of phase compensation for indoor positioning. Perfect cm-level localisation under temporal and dynamic conditions was also achieved with high bandwidth fingerprints (e.g. 300 MHz) using various localisation methods

Table 13 Recent survey papers on indoor positioning

Ref.	Positioning technique	Measured parameter	N/LOS?	Focused on CSI?	Focused on mobility?
[2]	ranging	ToA, TDoA	N/LOS	no	low
[63]	ranging	RSSI, ToA, TDoA, AoA	N/LOS	no	low
[1]	ranging	RSSI, ToA, TDoA, AoA	LOS	no	low
[64]	ranging	RSSI, ToA, TDoA	LOS	no	high
[8]	fingerprinting	RSSI	LOS	no	low
[7]	fingerprinting	RSSI	LOS	no	medium
[10]	fingerprinting	CSI	N/LOS	yes	low
[6]	fingerprinting, ranging	CSI	N/LOS	yes	low
[4]	fingerprinting, ranging etc.	CSI, RSSI, ToA, TDoA, AoA, velocity, image	N/LOS	no	low
[50]	dead reckoning, map matching	velocity, inertial measurements	LOS	no	high

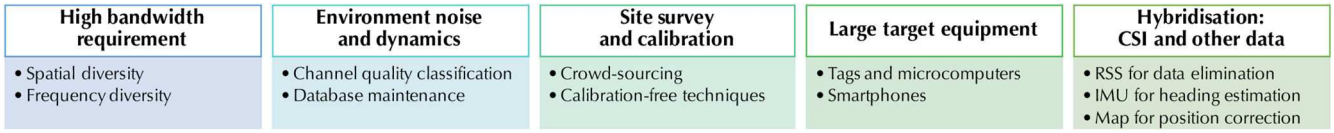

Fig. 16 *Summary of challenges and future directions of indoor positioning and tracking systems*

such as TRRS and SVM. However, positioning accuracy can go as low as 20% for low bandwidth cases when channel conditions were less than ideal (i.e. noisy channel). As a result, we have introduced a logistic regression classifier to sift out poor channels in a fingerprint and thereby to ensure the fingerprint quality in poor channel conditions. Fingerprint sifting can improve the performance of TRRS-based positioning by 8–73% and the performance of SVM-based positioning by 9–238%.

Experimental results in this survey corroborated the findings of other fingerprinting-based systems. In essence, we identified the following challenges for indoor localisation systems as shown in Fig. 16: high bandwidth requirement, environment conditions, database calibration, large equipment, and the need for hybridisation. High bandwidth fingerprints can be produced by spatial or frequency diversity. Solutions to temporal and dynamic variations include channel quality classification, frequent database maintenance, and theoretical modelling for calibration-free techniques. Crowd-sourcing of unlabelled CSI fingerprints could also be utilised for DNN training, which could alleviate the hassles of conventional site survey and database maintenance. Since CSI-based IPS require large tracked devices such as laptops and software radio peripherals, future works may transit towards portable devices like smartphones and consider combining multi-modal sensor data to rectify certain flaws of CSI fingerprinting.

7 Acknowledgment

This work was supported in part by the General Research Fund (Project No. 15201118) established under the University Grant Committee (UGC) of the Hong Kong Special Administrative Region (HKSAR), China; and by The Hong Kong Polytechnic University (Project No. G-YBXJ). The work of A. P.-T. Lau was supported in part by the National Key R&D Program of China (Project No. 2019YFB1803502).

8 References

[1] Deak, G., Curran, K., Condell, J.: 'A survey of active and passive indoor localisation systems', *Comput. Commun.*, 2012, **35**, (16), pp. 1939–1954
[2] Makki, A., Siddig, A., Saad, M., *et al.*: 'Survey of WiFi positioning using time-based techniques', *Comput. Netw.*, 2015, **88**, pp. 218–233
[3] Özsoy, K., Bozkurt, A., Tekin, I.: '2D indoor positioning system using GPS signals'. Proc. Int. Conf. on IPIN, Zurich, November 2010, pp. 1–6
[4] Oguntala, G., Abd-Alhameed, R., Jones, S., *et al.*: 'Indoor location identification technologies for real-time IoT-based applications: an inclusive survey', *Comput. Sci.Rev.*, 2018, **30**, pp. 55–79
[5] Huang, H., Zhou, J., Li, W., *et al.*: 'Wearable indoor localisation approach in Internet of Things', *IET Netw.*, 2016, **5**, (5), pp. 122–126
[6] Yang, Z., Zhou, Z., Liu, Y.: 'From RSSI to CSI: indoor localization via channel response', *ACM Comput. Surv.*, 2013, **46**, (2), pp. 25:1–25:32
[7] He, S., Chan, S.G.: 'Wi-Fi fingerprint-based indoor positioning: recent advances and comparisons', *IEEE Commun. Surv. Tutorials*, 2016, **18**, (1), pp. 466–490
[8] Hossain, A.K.M.M., Soh, W.S.: 'A survey of calibration-free indoor positioning systems', *Comput. Commun.*, 2015, **66**, pp. 1–13
[9] Youssef, M., Agrawala, A.: 'The Horus WLAN location determination system'. Proc. ACM Int. Conf. Mobisys, Seattle, WA, USA, June 2005, pp. 205–218
[10] Wang, B., Xu, Q., Chen, C., *et al.*: 'The promise of radio analytics: a future paradigm of wireless positioning, tracking, and sensing', *IEEE Signal Process. Mag.*, 2018, **35**, (3), pp. 59–80
[11] Ma, Y., Zhou, G., Wang, S.: 'WiFi sensing with channel state information: a survey', *ACM Comput. Surv.*, 2019, **52**, (3), pp. 46:1–46:36
[12] Bahl, P., Padmanabhan, V. N.: 'RADAR: an in-building RF-based user location and tracking system'. Proc. IEEE INFOCOM, Israel, March 2000, pp. 775–784
[13] Chapre, Y., Ignjatovic, A., Seneviratne, A., *et al.*: 'CSI-MIMO: indoor Wi-Fi fingerprinting system'. Proc. IEEE Int. Conf. on LCN, Edmonton, AB, Canada, September 2014, pp. 202–209
[14] Sanam, T.F., Godrich, H.: 'An improved CSI based device free indoor localization using machine learning based classification approach'. Proc. Conf. EUSIPCO, Rome, Italy, September 2018, pp. 2390–2394
[15] Sen, S., Radunovic, B., Choudhury, R.R., *et al.*: 'You are facing the Mona Lisa: spot localization using PHY layer information'. Proc. ACM Int. Conf. MobiSys, Lake District, UK, June 2012, pp. 183–196
[16] Chen, C., Chen, Y., Han, Y., *et al.*: 'Achieving centimeter-accuracy indoor localization on WiFi platforms: a frequency hopping approach', *IEEE IoT J.*, 2017, **4**, (1), pp. 111–121
[17] Großwindhager, B., Rath, M., Kulmer, J., *et al.*: 'SALMA: UWB-based single-anchor localization system using multipath assistance'. Proc. ACM. Conf. Sensys, Shenzhen, China, November 2018, pp. 132–144
[18] Wu, Z., Xu, Q., Li, J., *et al.*: 'Passive indoor localization based on CSI and naive Bayes classification', *IEEE Trans. Syst. Man Cybern., Syst.*, 2018, **48**, (9), pp. 1566–1577
[19] Wu, Z., Han, Y., Chen, Y., *et al.*: 'A time-reversal paradigm for indoor positioning system', *IEEE Trans. Veh. Technol.*, 2015, **64**, (4), pp. 1331–1339
[20] Chen, C., Chen, Y., Han, Y., *et al.*: 'Achieving centimeter accuracy indoor localization on WiFi platforms: a multi-antenna approach', *IEEE IoT J.*, 2017, **4**, (1), pp. 122–134
[21] Yu, H., Chen, G., Zhao, S., *et al.*: 'A passive localization scheme based on channel state information in an indoor environment'. Proc. Int. Conf. WAINA, Taipei, Taiwan, March 2017, pp. 576–580
[22] Brás, L., Pinho, P., Carvaloh, N.B.: 'Evaluation of a sectorised antenna in an indoor localisation system', *IET Microw. Antennas Propag.*, 2013, **7**, (8), pp. 679–685
[23] Wang, X., Gao, L., Mao, S., *et al.*: 'CSI-based fingerprinting for indoor localization: a deep learning approach', *IEEE Trans. Veh. Technol.*, 2017, **66**, (1), pp. 763–776
[24] Gan, X., Yu, B., Huang, L., *et al.*: 'Deep learning for weights training and indoor positioning using multi-sensor fingerprint'. Proc. IPIN, Sapporo, Japan, September 2017, pp. 1–7
[25] Potortì, F., Cassarà, P., Barsocchi, P.: 'Device-free indoor localisation with small numbers of anchors', *IET Wirel. Sens. Syst.*, 2018, **8**, (4), pp. 152–161
[26] Intel Ultimate N Wi-Fi Link 5300: Product Brief. Available at www/us/en/wireless-products/ultimate-n-wifi-link-5300-brief.html, accessed 22 April 2020
[27] Halperin, D., Hu, W., Sheth, A., *et al.*: 'Tool release: gathering 802.11n traces with channel state information', *ACM SIGCOMM Comput. Commun. Rev.*, 2011, **41**, (1), pp. 53–53
[28] Rocamora, J.M., Ho, I.W.H., Mak, M.W.: 'The application of machine learning techniques on channel frequency response based indoor positioning in dynamic environments'. Proc. IEEE Int. Conf. SECON (Workshops), Hong Kong, June 2018
[29] Rocamora, J.M., Ho, I.W.H., Mak, M.W.: 'Fingerprint quality classification for CSI-based indoor positioning systems'. Proc. ACM MobiHoc (PERSIST-IoT Workshop), Catania, Italy, July 2019, pp. 31–36
[30] IEEE Std 802.11n-2009: 'Wireless LAN medium access control (MAC) and physical layer (PHY) specifications amendment 5: enhancements for higher throughput', 2009
[31] Halperin, D., Hu, W., Sheth, A., *et al.*: 'Two antennas are better than one: a measurement study of 802.11n', University of Washington, 2009
[32] IEEE Std 802.11a-1999: 'Wireless medium access control (MAC) and physical layer (PHY) specifications: high speed physical layer in the 5 GHz band', 1999
[33] Chen, C., Chen, Y., Lai, H.Q., *et al.*: 'High accuracy indoor localization: a WiFi-based approach'. Proc. IEEE ICASSP, Shanghai, China, March 2016, pp. 6245–6249
[34] Magsino, E.R., Ho, I.W.H., Situ, Z.: 'The effects of dynamic environment on channel frequency response-based indoor positioning'. Proc. IEEE Int. Symp. on PIMRC, Montreal, QC, Canada, October 2017, pp. 1–6
[35] Kumar, D.P., Amgoth, T., Annavarapu, C.S.R.: 'Machine learning algorithms for wireless sensor networks: a survey', *Inf. Fusion*, 2019, **49**, pp. 1–25
[36] Mak, M.W.: 'Lecture 1 constrained optimization and support vector machines', Dept. of EIE, The Hong Kong Polytechnic University, 2018
[37] Lei, M., Huang, Y.: 'CFR and SNR estimation based on complementary Golay sequences for single-carrier block transmission in 60-GHz WPAN'. Proc. IEEEE WCNC, Budapest, Hungary, April 2009, pp. 1–5
[38] Rocamora, J.M.: 'Fingerprinting-based indoor positioning and mobility tracking systems using channel state information', Dept. of EIE, The Hong Kong Polytechnic University, 2018, unpublished report
[39] Ng, A.: 'Lecture 10 advice for applying machine learning', Coursera, 2018
[40] Xiao, J., Wu, K., Yi, Y., *et al.*: 'FIMD: fine-grained device-free motion detection'. Proc. IEEE ICPADS, Singapore, December 2012, pp. 229–235
[41] Gu, Y., Zhan, J., Ji, Y., *et al.*: 'MoSense: an RF-based motion detection system via off-the-shelf WiFi devices', *IEEE IoT J.*, 2017, **4**, (6), pp. 2326–2341
[42] Liu, J., Wang, L., Guo, L., *et al.*: 'A research on CSI-based human motion detection in complex scenarios'. Proc. IEEE Int. Conf. Healthcom, Dalian, China, October 2017, pp. 1–6
[43] Zhang, F., Chen, C., Wang, B., *et al.*: 'A time-reversal spatial hardening effect for indoor speed estimation'. Proc. IEEE Int. Conf. ICASSP, New Orleans, LA, USA, March 2017, pp. 5955–5959

[44] Zhang, F., Chen, C., Wang, B., *et al.*: 'WiBall: a time-reversal focusing ball method for decimeter-accuracy indoor tracking', *IEEE IoT J.*, 2018, **5**, (5), pp. 4031–4041
[45] Xu, C., Firner, B., Zhang, Y., *et al.*: 'Improving RF-based device-free passive localization in cluttered indoor environments through probabilistic classification methods'. Proc. ACM/IEEE IPSN, Beijing, China, April 2012, pp. 209–220
[46] Shi, S., Sigg, S., Chen, L., *et al.*: 'Accurate location tracking from CSI-based passive device-free probabilistic fingerprinting', *IEEE Trans. Veh. Technol.*, 2018, **67**, (6), pp. 5217–5230
[47] Zhang, F., Chen, C., Wang, B., *et al.*: 'WiSpeed: a statistical electromagnetic approach for device-free indoor speed estimation', *IEEE IoT J.*, 2018, **5**, (3), pp. 2163–2177
[48] Zhao, Y., Patwari, N., Phillips, J.M., *et al.*: 'Radio tomographic imaging and tracking of stationary and moving people via kernel distance'. Proc. ACM/IEEE IPSN, PA, USA, April 2013, pp. 229–240
[49] Wu, K., Xiao, J., Yi, Y., *et al.*: 'FILA: fine-grained indoor localization'. Proc. IEEE INFOCOM, FL, USA, March 2012, pp. 2210–2218
[50] Yang, Z., Wu, C., Zhou, Z., *et al.*: 'Mobility increases localizability: a survey on wireless indoor localization using inertial sensors', *ACM Comput. Surv.*, 2015, **47**, (3), pp. 54:1–54:34
[51] Schüssel, M.: 'Angle of arrival estimation using WiFi and smartphones'. Proc. IPIN, Alcalá de Henares, Spain, October 2016, pp. 1–4
[52] Zhang, Y., Zhang, L.: 'WiFi-based contactless activity recognition on smartphones'. Proc. IEEE/CIC ICCC, Qingdao, China, October 2017, pp. 1–6
[53] Jachimczyk, B., Dziak, D., Kulesza, W.J.: 'RFID – hybrid scene analysis-neural network system for 3D indoor positioning optimal system arrangement approach'. Proc. IEEE I2MTC, Montevideo, Uruguay, May 2014, pp. 191–196
[54] Chuenurajit, T., Phimmasean, S., Cherntanomwong, P.: 'Robustness of 3D indoor localization based on fingerprint technique in wireless sensor networks'. Proc. Int. ECTI-CON, Krabi, Thailand, May 2013, pp. 1–6
[55] Fang, B., Lane, N.D., Zhang, M., *et al.*: 'BodyScan: enabling radio-based sensing on wearable devices for contactless activity and vital sign monitoring'. Proc. ACM Int. Conf. MobiSys, Singapore, June 2016, pp. 97–110
[56] Fang, B., Lane, N.D., Zhang, M., *et al.*: 'HeadScan: a wearable system for radio-based sensing of head and mouth-related activities'. Proc. ACM/IEEE IPSN, Vienna, Austria, April 2016, pp. 1–12
[57] Xie, Y., Li, Z., Li, M.: 'Precise power delay profiling with commodity WiFi'. Proc. ACM Mobicom, Paris, France, September 2015, pp. 53–64
[58] 'Nexmon: the C-based firmware patching framework', Available at https://nexmon.org, accessed 11 March 2020
[59] Herrera, J.C.A., Plöger, P.G., Hinkenjann, A., *et al.*: 'Pedestrian indoor positioning using smartphone multi-sensing, radio beacons, user positions probability map and indoorOSM floor plan representation'. Proc. IPIN, Busan, South Korea, October 2014, pp. 636–645
[60] Noertjahyana, A., Wijayanto, I.A., Andjarwirawan, J.: 'Development of mobile indoor positioning system application using android and bluetooth low energy with trilateration method'. Proc. ICSIIT, Denpasar, Indonesia, September 2017, pp. 185–189
[61] Pradhan, S., Baig, G., Mao, W., *et al.*: 'Smartphone-based acoustic indoor space mapping', *Proc. ACM Interact. Mob. Wearable Ubiquitous Technol.*, 2018, **2**, (2), pp. 75:1–75:26
[62] Li, M., Meng, Y., Liu, J., *et al.*: 'When CSI meets public WiFi: inferring your mobile phone password via WiFi signals'. Proc. ACM SIGSAC Conf. on CCS, Vienna, Austria, October 2016, pp. 1068–1079
[63] Gezici, S., Tian, Z., Giannakis, G.B., *et al.*: 'Localization via ultra-wideband radios: a look at positioning aspects for future sensor networks', *IEEE Signal Process. Mag.*, 2005, **22**, (4), pp. 70–84
[64] Halder, S., Ghosal, A.: 'A survey on mobility-assisted localization techniques in wireless sensor networks', *J. Netw. Comput. Appl.*, 2016, **60**, pp. 82–94